Speciation of the Fe(II)–Fe(III)–H_2SO_4–H_2O system at 25 and 50 °C

J.M. Casas [a,*], G. Crisóstomo [b], L. Cifuentes [b]

[a] *Departamento de Ingeniería Química, Universidad de Chile, Av. Beauchef 861, Santiago, Chile*
[b] *Departamento de Ingeniería de Minas, Universidad de Chile, Av. Tupper 2069, Santiago, Chile*

Abstract

This work presents theoretical and experimental results on the speciation of the Fe(II)–Fe(III)–H_2SO_4–H_2O system in concentrated solutions (up to 2.2 m H_2SO_4 and 1.3 m Fe). The aim was to study the chemical equilibria of iron at 25 and 50 °C in synthetic aqueous sulphuric acid solutions that contain dissolved ferric and ferrous ion species. Raman spectroscopy, volumetric titration and conductivity measurements have been carried out in order to study the presence of specific ions and to characterize the ionic equilibrium. A thermochemical equilibrium model incorporating an extended Debye–Hückel relationship was used to calculate the activities of ionic species in solution. Model calculations were compared with experimental results. Model simulations indicate that anions, cations and neutral complexes coexisted in the studied system, where the dominant species were HSO_4^-, H^+, Fe^{2+} and $FeH(SO_4)_2^0$. This indicated that these solutions showed a high buffer capacity due to the existence of bisulphate ions (HSO_4^-), which presented the highest concentration. A decrease in the concentration of H^+ and Fe^{3+} took place with increasing temperature due to the formation of complex species. Standard equilibrium constants for the formation of $FeH(SO_4)_2^0$ were obtained in this work: $\log K_f^0 = 8.1 \pm 0.3$ at 25 °C and 10.0 ± 0.3 at 50 °C.

Keywords: Iron; Ferrous; Ferric; Equilibrium model; Speciation; Sulphuric acid; Ionic conductivity; Equilibrium constants; Rhomboclase

1. Introduction

1.1. Previous work

Dissolved and precipitated iron compounds are relevant in many metallurgical processes. For example, iron compounds are by-products in the zinc and copper industries, which are obtained from the dissolution of limonite ($FeOOH^*nH_2O$) or sulphide minerals such as pyrite (FeS_2), pyrrhotite (FeS), chalcopyrite ($CuFeS_2$), and bornite (Cu_5FeS_4). In mineral and aqueous compounds iron exists in the 0, +2 and +3 oxidation states (Lide, 1999; Langmuir, 1997). During the last 40 years a great number of scientific studies have been performed with iron solutions to measure and to evaluate the solubility, the speciation and the kinetics of mineral leaching, precipitation and crystallization, where this metal participated (Linke, 1958; Dutrizac and MacDonald, 1974; Dutrizac and Harris, 1996; Dutrizac and Monhemius, 1986; Tozawa and Sasaki, 1986; Dry and Bryson, 1988; Barrett et al., 1993; Swash and Monhemius, 1994; Rao et al., 1995; Stumm and Morgan, 1996; Butler and Cogley, 1998; Welham et al., 2000; Roine, 2002; Cifuentes et al., 2003; Casas et al., 2005). In aqueous sulphuric acid solutions iron distributes as dissolved Fe(II) and Fe(III) species (oxidation states +2 and +3, respectively), as free ions (Fe^{3+}, Fe^{2+}) or complex compounds [$FeSO_4^0$, $FeSO_4^+$,

* Corresponding author. Fax: +56 2 6991084.
Email addresses: jecasas@ing.uchile.cl (J.M. Casas), luicifue@ng.uchile.cl (L. Cifuentes).

$Fe(SO_4)_2^-$]. The concentration of these species is strongly dependent on solution composition and temperature. Corresponding aqueous equilibrium reactions are summarized as follows (Dutrizac and Harris, 1996; Barrett et al., 1993; Stumm and Morgan, 1996; Langmuir, 1997):

$$Fe^{2+} + SO_4^{2-} \Leftrightarrow FeSO_4^0$$

$$Fe^{3+} + SO_4^{2-} \Leftrightarrow FeSO_4^+$$

$$Fe^{3+} + 2SO_4^{2-} \Leftrightarrow Fe(SO_4)_2^-$$

$$H^+ + SO_4^{2-} \Leftrightarrow HSO_4^-$$

Depending on solution concentration and temperature a large number of iron minerals could precipitate in the mentioned system, such as: hematite (Fe_2O_3), magnetite (Fe_3O_4), goethite (FeOOH), hydrous ferric oxides ($Fe_2O_3^*nH_2O$), brucite [$Fe(OH)_2$], hydronium jarosite [$H_3OFe_3(SO_4)_2(OH)_6$], schwertmannite ($Fe_8O_8(OH)_6SO_4$), melanterite ($Fe_2SO_4^*7H_2O$), rozenite ($FeSO_4{\cdot}4H_2O$), szomolnokite ($Fe_2SO_4^*H_2O$), rhomboclase [$FeH(SO_4)_2$], coquimbite [$Fe_2(SO_4)_3$*$9H_2O$], cornelite [$Fe_2(SO_4)_3$*$7H_2O$], iron–hydroxy-sulfates [$Fe_x(SO_4)_y(OH)_z$], among others (Linke, 1958; Dutrizac and Harris, 1996; Stumm and Morgan, 1996; Langmuir, 1997; Welham et al., 2000).

The speciation of iron in natural and industrial environments, as well as iron separation and control in metallurgical processes, has undergone tremendous improvements during the last decades (Dutrizac and Harris, 1996; Dry and Bryson, 1988; Senanayake and Muir, 1988; Swash and Monhemius, 1994; Rao et al., 1995; Stumm and Morgan, 1996; Das and Krishna, 1996; Marconi et al., 1996; Langmuir, 1997; Butler and Cogley, 1998; Cifuentes et al., 1999; Welham et al., 2000). However, only limited thermodynamic information regarding iron species, which are present in concentrated sulphuric acid solutions, can be derived from reported experiments and available geochemical databases. Moreover, most of the studies were carried out in diluted systems, while complete thermochemical data derived from iron sulphate solubility in aqueous sulphuric acid systems are unavailable.

1.2. Objectives

The aim of this work is to study, from both experimental and theoretical points of view, the chemical equilibrium and speciation of iron at 25 and 50 °C in synthetic aqueous sulphuric acid solutions that contain dissolved ferric and ferrous ion species. Systems to be studied correspond to: Fe(II)–Fe(III)–H_2SO_4–H_2O, with 2.2 m H_2SO_4 and 0–1.3 m Fe.

A thermodynamic model was developed to quantify the speciation of aqueous iron–sulphate compounds at various concentrations. Model calculations are compared with experimental results.

2. Experimental methodology

Experimental work to study the iron(III) speciation in the Fe(II)–Fe(III)–H_2SO_4–H_2O system was carried out by preparing a set of solutions formed by ferrous sulphate, ferric sulphate, sulphuric acid and water. Experiments were performed for 3 h using an orbital shaker with 250 cm^3 glass shake flasks. Solutions were equilibrated in agitated beakers at 25 and 50±0.5 °C, and then liquid samples were taken and filtered at room temperature with 0.1 μm Millipore® membrane filter. Chemical analyses were performed to determine the concentration of total iron as Fe(tot) and Fe(II). Solution density, pH, and ionic conductivity were measured.

The analytical procedure was as follows: distilled water was used throughout, solution samples were measured in duplicate and the reproducibility was ±1%. The stock solution of sulphuric acid was prepared by dilution of the concentrated analytical reagent (H_2SO_4 95–97%, p.a., Merk®) and titrisol 0.5 M H_2SO_4 (No 1.09981, Merck®).

The iron reagents used were: $FeSO_4^*7H_2O$ (99% purity, Fluka® Chemie A.G.), and $FeH(SO_4)_2$ (98% purity Aldrich® Chem. Co.). The concentration of total dissolved iron [Fe(tot)], was determined by atomic absorption spectroscopy at λ 296.7 nm for low levels and λ 305.9 nm for high levels with a precision of ±0.5%, using a Perkin Elmer® 1100B spectrophotometer. The concentration of ferrous iron [Fe(II)] was determined by modified ortho-phenanthroline method (Herrera et al., 1989), using visible spectrophotometry at 510 nm with a precision of ±2%, using a Perkin Elmer® Lambda 1 spectrophotometer.

Solution densities were determined by means of a 10 cm^3 glass pycnometer and an analytical digital balance (PRECISA® XB22A), with a precision of 0.0001 g. The values of pH of the solution were measured with a Jenway® meter, model 4350, using a combination electrode with Ag/AgCl (No. 924005, Jenway®). The ionic conductivity of the solution was determined with a reproducibility of 5–10% using a Jenway® meter and a glass platinum cell of 1.3 cm^{-1}, which works in the range of 1×10^{-4} to 2000 mS/cm. The conductivity cell was calibrated at 25 and 50 °C,

using standard sulphuric acid solutions for the 100–1100 mS/cm range, depending on the conductivity interval of the tested solutions.

Raman vibrational spectroscopy was carried out with a Jobin–Yvon® spectrophotometer by using the 632.8 nm excitation line, provided by a He–Ne laser. The liquid samples were placed in a Petri dish and mounted in an Olympus® BX-40 microscope (objective ×10), taking one scan with an integration time of 150 s. The solid samples were placed on a glass slide and analysed with the ×100 objective of the microscope using a filter to screen 99% of the laser incident light to prevent sample alteration, and then taking one scan with an integration time of 300 s.

Molality was used as concentration unit (mol/kg H_2O) in order to allow for solution density effects.

3. Modelling

Aqueous speciation in multi-component ionic systems can be determined by the application of a thermodynamic model which consists of a set of defined species, components and reactions, plus a set of equilibrium relationships and mass balance equations for each defined component. This calculation methodology was presented in previous articles (Casas et al., 2000, 2003). The electrolyte speciation in aqueous solutions can be estimated using appropriate ionic activity coefficient models, depending on the solution concentration (Helgeson et al., 1981; Zemaitis et al., 1986; Rafal et al., 1994; Wolery, 1996; Grenthe and Plyasunov, 1997).

In the case of electrolytic solutions at moderate concentrations (0.3 to 1.5 m), the main models that could be applied are: extended Debye–Hückel (Helgeson et al., 1981; Wolery, 1996; Casas et al., 2003), Bromley–Zemaitis (Zemaitis et al., 1986; Rafal et al., 1994), and specific interaction (Grenthe and Plyasunov, 1997). In the present work, the extended Debye–Hückel model is used to evaluate the activity coefficients (γ_i) of dissolved species in the system. This model has been shown to produce good results in solutions in similar aqueous-sulphuric acid-metal systems (Helgeson et al., 1981; Cifuentes et al., 2002, 2003), which indicates its suitability for the present study. A detailed speciation modelling methodology is presented by Stumm and Morgan, 1996. The main relationships are:

Equilibrium:

$$K_{ri} = \prod_{j=1}^{N_{sp,ri}} a_j^{\pm \nu_j} \tag{1}$$

Mass balance:

$$\text{TOT } X_j = \sum_{i=1}^{N_{sp}} \nu_i m_i \tag{2}$$

where K_{ri}, is the equilibrium constant of reaction for the formation of the i-th species; m_i, a_i and $\pm\nu$ are the molal concentration, the activity, and the stoichiometric coefficient (+ for products and − for reactants) of the i-th species, respectively. TOT X_j is the total molal concentration of the j-th component. Activity and concentration are related by $a_i = m_i \cdot \gamma_i$, where γ_i is the activity coefficient of the i-th species (see units in Notation section below).

The extended Debye–Hückel model is represented as:

$$\log(\gamma_i) = \frac{-Az_i^2\sqrt{I}}{1 + \mathring{a}_i B\sqrt{I}} + \dot{B} \cdot I \tag{3}$$

Eq. (3) is also known as the B-dot equation; $\mathring{a}_i$ is the hard-core diameter of the i-th ionic species, z_i is the charge of the i-th species, A and B are Debye–Hückel parameters and I is the solution ionic strength. This model has three temperature dependent parameters (A, B and $\dot{B}$), as shown in Table 1, and one parameter for each of the solvated species, the "hard-core diameter" ($\mathring{a}$). This is a modification of the classical Debye–Hückel model and it is valid for binary interactions. In order to correct the activity coefficient for those cases where molecular interactions—other than electrostatic ones—come into play, the same value in the B-dot parameter is included for all participating species. The model is valid for aqueous electrolyte solutions with moderate ionic strength values. The validity range for this model has been reported up to $I = 1$ m (Helgeson et al., 1981; Wolery, 1996; Casas et al., 2003). The term $\dot{B} \cdot I$ represents a correction for short-range interactions. The extended Debye–Hückel model has been used by Helgeson and coworkers and introduced in several

Table 1
Extended Debye–Hückel parameters at 25 and 50 °C (Wolery, 1996)

Parameter	Temperature	
	25 °C	50 °C
A ($kg^{0.5}/mol^{0.5}$)	0.5114	0.5365
B ($kg^{0.5}/mol^{0.5}/Å$)	0.3288	0.3329
$\dot{B}$ (kg/mol)	0.0410	0.0430

Table 2
Experimental measurements for the Fe(II)–Fe(III)–H_2SO_4–H_2O system at 25±0.2 °C and 50±0.2 °C

[Fe(II)] (g/L)	[Fe(tot)] (g/L)	Density at 25 °C (g/cm^3)	Solution conductivity at 25 °C (mS/cm)	Solution conductivity at 50 °C (mS/cm)
System Fe(II)–H_2SO_4–H_2O				
0.00	0.00	1.1159	667	1039
5.05	5.55	1.1290	582	904
14.00	14.20	1.1464	542	780
28.02	28.70	1.1781	493	715
42.25	43.40	1.2042	444	618
55.66	56.40	1.2323	403	542
77.26	78.00	1.2814	330	456
System Fe(III)–H_2SO_4–H_2O				
0.003	4.47	1.1309	639	1002
0.005	10.80	1.1509	596	918
0.006	21.30	1.1837	547	812
0.009	32.40	1.2152	493	720
0.011	43.10	1.2483	450	634
0.014	53.80	1.2773	401	553
0.016	65.40	1.3113	355	489
System Fe(II)–Fe(III)–H_2SO_4–H_2O				
2.38	5.0	1.1298	626	939
6.17	12.2	1.1498	596	883
13.25	25.1	1.1799	546	784
21.15	37.6	1.2024	490	680
27.11	50.1	1.2393	446	593
35.18	71.6	1.2874	366	489

speciation codes and geochemical software, such as: MINTEQA2 (Allison et al., 1991); PHREEQC (Parkhurst, 1995), and EQ3/6 (Wolery, 1996).

A rigorous methodology was applied to validate the speciation. First, the model was defined by selecting an appropriate ion activity model and a list of main species according to the published literature and measurements obtained by laser Raman spectroscopy. Second, the model was calibrated using revised equilibrium constant values for the selected iron species and the supporting electrolyte (sulphuric acid). Solubility data for the rhomboclase as a function of pH was used to obtain the equilibrium constant for $FeH(SO_4)_2^0$ by mathematical regression. Third, the model was validated on the basis of solution conductivity measurements using independent sets of experimental data, which correspond to an indirect determination of iron speciation in the studied solutions.

4. Results and discussion

4.1. Experimental results

Experimental results of the speciation study performed by chemical analysis of aqueous solutions containing sulphuric acid and iron sulphates are shown in Table 2 and Figs. 1 and 2.

Table 2 presents solution density and conductivity of Fe(II)–Fe(III)–H_2SO_4–H_2O systems in the following conditions: 2.2 m H_2SO_4, 0–1.3m Fe, at temperatures 25 and 50 °C.

A decrease in conductivity is observed when temperature decreases and iron concentration increases. The conductivity of aqueous sulphuric acid solutions that contain dissolved metals is mainly determined by the concentration of hydrogen ion (H^+), (Casas et al., 2000, 2003), because this ion exhibits the highest mobility.

Fig. 1 and Table 3 show respectively the Raman spectra and the bands assigned to aqueous solutions formed by mixtures of H_2SO_4 and $FeH(SO_4)_2$. The

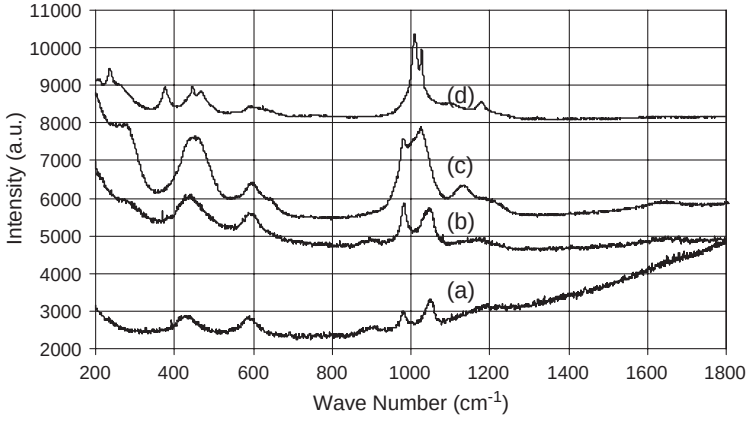

Fig. 1. Laser Raman spectra of solutions: (a) 2.22 m $H_2SO_4+H_2O$; (b) 0.64 m $FeH(SO_4)_2^0$+2.22 m $H_2SO_4+H_2O$; (c) 1.09 m $FeH(SO_4)_2^0$+2.22 m $H_2SO_4+H_2O$; (d) solid reagent $FeH(SO_4)_2$.

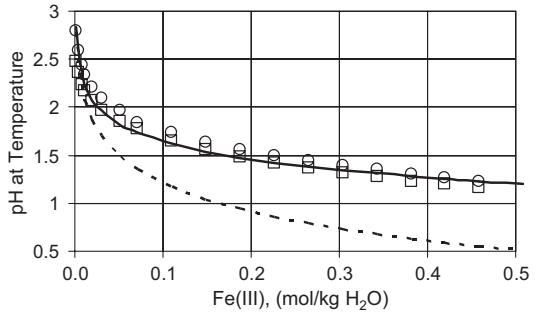

Fig. 2. Equilibrium pH of solutions formed by dissolution of rhomboclase [$FeH(SO_4)_2$] in water as a function of Fe(III) concentration. Experimental data; o: 25 °C and □: 50 °C. Model predictions : — including $FeH(SO_4)_{2(aq)}$ species and —- without $FeH(SO_4)_{2(aq)}$ species.

figure presents the spectra of the supporting electrolyte (2.2 m sulphuric acid solution) and iron solutions, as well as the spectra of the pure reagents (solid iron compounds).

The band at 985 cm^{-1} corresponds to S–O stretching vibrations, indicating the presence of sulphate. In this case sulphate displays tetrahedral coordination geometry. When an iron sulphate salt is dissolved in water, sulphate ions (the ligands) show some distortion of their tetrahedron-type geometry due to the presence of counter ion interaction; in this case the spectrum shows a frequency shift for the band in the 910–920 cm^{-1} range [$\nu_1(SO_4^{2-})$ symmetric stretching] and in the 984–1210 cm^{-1} range [$\nu_3(SO_4^{2-})$ asymmetric stretching]. The triple degeneration of ν_3 is high with its corresponding unfolding in 2 or 3 bands, depending on the symmetry of the formed structure (Nakamoto, 1997). This effect reveals the presence of bisulphate ions in solution (HSO_4^-), the relative intensity of the mentioned bands increases with solution concentration.

Table 3
Raman spectral bands assignment in the Fe(II)–Fe(III)–H_2SO_4–H_2O system (Nakamoto, 1997)

Band range (cm^{-1})	Molecular interaction
242–276	ν(Fe–O)
373–382	ν(Fe–O)
440–475	$\nu_2(SO_4^{2-})$
596–620	$\nu_4(SO_4^{2-})$
910–920	$\nu_1(SO_4^{2-})$
984–1013	$\nu_1(SO_4^{2-})$
1030–1098	$\nu_3(SO_4^{2-})$
1140–1210	$\nu_3(SO_4^{2-})$
1628–1680	H_2O bending

Sulphate vibration modes ν_1: symmetric; stretching, ν_2: bending, ν_3: asymmetric stretching, ν_4: bending.

Evidence of the interaction between dissolved iron ions and sulphate appears in the 440–620 cm^{-1} and 1140–1210 cm^{-1} ranges, which correspond to bending and asymmetric stretching vibrations, respectively (Nakamoto, 1997). The bands in the 242–282 cm^{-1} range are attributed to vibrations of Fe–OH–S which suggests the presence of neutral $FeH(SO_4)_2^0$ species. These start to be detected at concentrations over 0.64 m. A summary of spectral band assignment is presented in Table 3.

Fig. 2 shows experimental results for pH at 25 and 50 °C in solutions formed by the dissolution of the rhomboclase (acid iron sulphate) in deionised water. These measurements show that solution pH decreases from about 2.5 to 1.25 as Fe(III) concentration increases from 2×10^{-3} to 0.5 m, which is explained by the increase in solution acidity according to the reaction:

$$FeH(SO_4)_2^0 \Leftrightarrow Fe^{3+} + H^+ + 2SO_4^{2-}$$

For the studied conditions, a small effect of temperature was observed: iron hydrolysis is favoured by increasing temperature, producing a slight decrease in the pH value of the solution. Results of these experiments were used to calibrate and validate the speciation model according the results present below.

4.2. Modelling results

The developed thermodynamic model was used to study the speciation (i.e., the distribution and concentration of dissolved species) in aqueous solutions which contain sulphuric acid and dissolved iron, at 25 and 50 °C. The used model implements an extended Debye–Hückel formalism and is analogous to the one described in detail in previous articles (Casas et al., 2000,

Table 4
Stoichiometry of the main species as a function of components in the Fe(II)–Fe(III)–H_2SO_4–H_2O system

Species	Components					Log K_f^o, 25°C	Log K_f^o, 50°C	Ref.
	H_2O	H^+	SO_4^{2-}	Fe^{2+}	Fe^{3+}			
HSO_4^-	0	1	1	0	0	1.98	2.32	(1)
$FeSO_4^0$	0	2	0	1	0	2.25	2.44	(2,3)
$Fe(SO_4)_2^-$	0	0	2	0	1	5.38	7.64	(2,3)
$FeSO_4^+$	0	0	1	0	1	4.04	4.76	(2,3)
$FeH(SO_4)_2^0$	0	1	2	0	1	8.10	10.00	(*)
Molality	55.51	4.4	2.2–3	0–1	0–1			

1: Shock (1998).
2: Stumm and Morgan (1996).
3: Roine (2002).
*: Calculated from solubility data of rhomboclase in this work.

2003, 2005; Cifuentes et al., 2002). Table 4 summarizes the speciation model and calculation results are presented in Fig. 3 and 4. Dissolved iron species were selected from the data published by Stumm and Morgan (1996), Langmuir, 1997, and Welham et al. (2000). Iron bisulphate ions like $FeHSO_4^+$ and $FeHSO_4^{2+}$ were not considered in this speciation model due to the evidence reported by Tremaine et al. (2004), who studied the Fe–H_2O–H_2SO_4 system using Raman spectroscopy and did not find any evidence of contact ion pairs between $HSO_{4\,(aq)}^-$ and iron cations, and explained that the bisulphate is a non-complexing anion. Model calculations are compared with the present experimental data and results published by other workers (Baes and Mesmer, 1976; Ryzhenko et al., 1985; Stumm and Morgan, 1996; Shock, 1998; Roine, 2002).

4.2.1. Model calibration

In the present work, the equilibrium constant approach is adopted to model the solution equilibrium because standard equilibrium constants are the key parameters for the speciation model. The model formulation that represents the aqueous speciation in the Fe–H_2O–H_2SO_4 system is summarised in the Table 4 as a "speciation tableau", where reactions are represented as stoichiometric combinations of components. The aqueous species were selected from the literature (Stumm and Morgan, 1996; Roine, 2002).

The neutral $FeH(SO_4)_2^0$ species must be incorporated in the model to fit the ferric sulphate solubility data. The existence of these species was demonstrated by the results obtained by Raman spectroscopy presented above and calculations shown in Fig. 2. This figure shows that, if the $FeH(SO_4)_2^0$ is not included, the model fails to predict the pH, while its inclusion leads to agreement with measurements carried our for the Fe (III)–SO_4–H_2O system.

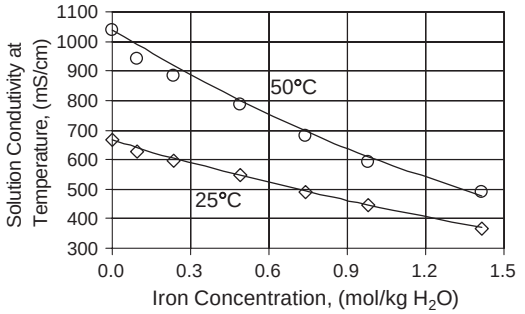

Fig. 4. Solution conductivity at 25 and 50 °C as a function of ferric plus ferrous iron concentration in aqueous solution with 2.22 m H_2SO_4. Experimental data; ◇: 25 °C and ○: 50 °C. Model predictions: —.

The system can be evaluated by the following set of mass balance equations for each defined component:

$$H(tot) = [H^+] + [HSO_4^-] + [FeH(SO_4)_2^0] \quad (4)$$

$$SO_4(tot) = [SO_4^{2-}] + [HSO_4^-] + [FeSO_4^+] + [FeSO_4^0] + 2*[Fe(SO_4)_2^-] + 2*[FeH(SO_4)_2^0] \quad (5)$$

$$Fe(II) = [Fe^{2+}] + [FeSO_4^0] \quad (6)$$

$$Fe(III) = [Fe^{3+}] + [FeSO_4^+] + [Fe(SO_4)_2^-] + [FeH(SO_4)_2^0] \quad (7)$$

To solve the balance equations, 4 concentrations must be fixed in advance: those of H(tot), SO_4(tot), Fe (II) and Fe(III), that correspond to selected system components.

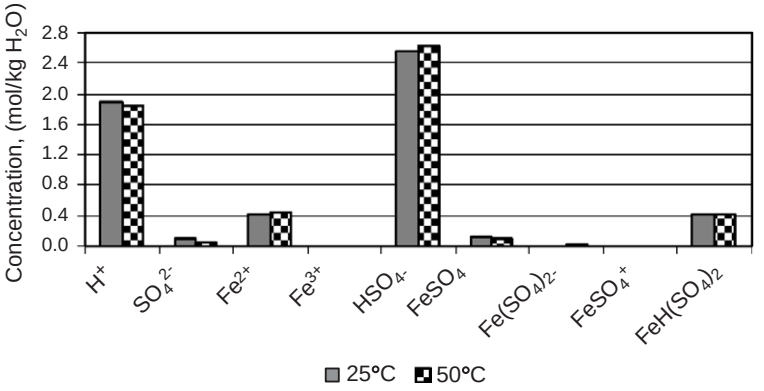

Fig. 3. Calculated speciation at 25 and 50 °C for an aqueous solution containing: [H_2SO_4]=2.22 m (200 g/L); [Fe(II)]=0.543 m (27 g/L); [Fe(III)]=0.437 m (23 g/L).

In summary, the equilibrium speciation model used in this work consists of an algebraic non-linear system formed by a set of mass balance equations for each defined component, the equilibrium relationships and the ionic activities {Eq. (1)–(3)}. A computer program developed with the Matlab® software was used to solve the model equations. This program implements a multi-dimensional Newton–Raphson numerical algorithm and allows the calculation of the aqueous multi-component speciation in the presence of ions, complexes and solid species for a wide range of solution concentration values.

Model calibration was obtained first by using revised standard equilibrium constants of iron complexes at 25 and 50 °C; the selected values are presented in Table 4. Data at 50 °C were estimated using the heat capacity integration method and calculations were performed with the help of the HSC-Chemistry software (Roine, 2002). Then, as a second calibration step, solubility data obtained from the dissolution of rhomboclase (acid iron sulphate) in water were selected to estimate the standard equilibrium constants for the aqueous neutral species $FeH(SO_4)_2^0$. These key-value parameters were obtained by fitting the model to experimental data for solution pH as a function of Fe(III) concentration. Mathematical regression was carried out by minimising the sum of squares of the differences between experimental and calculated data presented by Fig. 2. The *K*-values obtained for this species were: $\log K^0_{f\,FeH(SO4)2(aq)} = 8.1 \pm 0.3$ at 25 °C and 10.0 ± 0.3 at 50 °C.

4.2.2. Model calculations

Thermodynamic simulations for the speciation of the Fe(II)–Fe(III)–H_2SO_4–H_2O system were carried out at 25 and 50 °C. Fig. 3 shows the results of the equilibrium calculation for an aqueous solution formed by 2.22 m H_2SO_4 (200 g/L), 0.543 m Fe(II) (27 g/L), and 0.437 m Fe(III) m (23 g/L).

A decrease in the concentration of free ions was observed as temperature increased due to the increased stability of HSO_4^- and $Fe(SO_4)_2^-$ species with temperature. Fe(II) species distribute as 78–83% $Fe^{2+}$and 22–17% $FeSO_4^0$. Fe(III) species distribute as 96.6–93.9% $FeH(SO_4)_2^0$, 2.1–5.9% $Fe(SO_4)_2^-$, and 1.3–0.2% $FeSO_4^+$. Sulphate species distribute as 70.2–72.2% HSO_4^-, 23.2–22.5% $FeH(SO_4)_2^0$, and 3.3–2.5% $FeSO_4^0$, 2.6–1.4% SO_4^{2-} and 0.5–1.4% $Fe(SO_4)_2^-$. Hydrogen species distribute as 52–54% HSO_4^-, 39–38% H^+, 9–8% and $FeH(SO_4)_2^0$.

Model simulations indicate that anions, cations and neutral complexes are present in the concentrated Fe (II)–Fe(III)–H_2SO_4–H_2O system. Dominant species in the studied conditions were HSO_4^-, H^+, $Fe^{2+}$and $FeH(SO_4)_2^0$, which indicates that this solution presents a high buffer capacity due to the existence of bisulphate ions (HSO_4^-) as main species. The concentration of free ferric ion (Fe^{3+}) is very low and Fe(III) distributes mainly as $FeH(SO_4)_2^0$ and $Fe(SO_4)_2^-$ species. The concentration of free ferrous ion (Fe^{2+}) is very high and Fe(II) distributes mainly as $Fe^{2+}$and $FeSO_4^0$ species.

4.2.3. Model validity

The inclusion of $FeH(SO_4)_2^0$ species in the speciation model is validated according to the Raman spectra observations and model calculations presented by Figs. 1 and 2, respectively.

A comparison between conductivity measurements and model calculations was used to validate the thermodynamic speciation model (Anderko and Lencka, 1997; Sperry and Nagy, 1998; Baghalha and Papangelakis, 2000; Casas et al., 2000, 2003). The conductivity of the solution was calculated as:

$$\kappa = \frac{F^2}{RT}\sum_{i}^{NI} z_i^2 C_i D_{ef,i} \tag{8}$$

where κ is the solution conductivity measured with a conductivity cell (mS/cm), F is Faraday's constant, R is the ideal gas constant, T is the absolute temperature, NI is the number of ionic species, and z_i, C_i and $D_{ef,i}$, are the ionic charge, the molar concentration and the effective diffusivity of the ionic species "*i*" in solution, respectively.

At present, no theoretical methods are available for predicting the conductivity of concentrated solutions that contain several ions, therefore the use of Eq. (8) demands knowledge of ion concentrations and their diffusivities in aqueous solution. Ionic concentrations can be calculated with the help of the speciation model and the effective diffusivity ($D_{ef,i}$) must be determined via mathematical regression from experimental data for multi-component solutions.

It is known that hydrogen ions are the most mobile species in solution, so the following approximation was introduced to obtain a relationship between hydrogen ion diffusivity and solution conductivity:

$$\kappa = \frac{F^2}{RT} D_{ef,H^+}\left[C_{H^+} + \sum_{i}^{NI-1} z_i^2 C_i \frac{D_{ef,i}}{D_{ef,H^+}}\right] \tag{9}$$

Then, the effective diffusivity ratios are approximated by standard diffusivity ratios at 25 °C, which are known for diluted solutions, as follows:

$$\frac{D_{\mathrm{ef},i}}{D_{\mathrm{ef},H^+}} \approx \frac{D_i^0}{D_{H^+}^0} \tag{10}$$

For the case of the complex ions, the standard diffusivity was calculated according to the methodology proposed by Anderko and Lencka (1997) for multi-electrolyte solutions as follows:

$$D_{\mathrm{complex}}^0 = \frac{|Z_{\mathrm{complex}}|}{\left[\sum_{j=1}^{NC}\left(\frac{z_j}{D_j^0}\right)^3\right]^{1/3}} \tag{11}$$

Table 5 shows the standard diffusivities of ionic species at 25 °C calculated for iron sulphate complexes using the Eq. (11) and the ionic conductivities of the free ions reported by Lide (1999).

Finally, the effective diffusivity of hydrogen ions was corrected for solution concentration using an empirical relationship, developed by the authors, which was then fitted to experimental data for the studied systems, the proposed model is:

$$D_{\mathrm{ef},H^+} = D_{H^+}\exp\left(-\frac{m_{\mathrm{Fe}}}{m_{\mathrm{H}}^{\mathrm{ref}}}\right) \tag{12}$$

where D_{H+} is the hydrogen ion diffusivity in the supporting electrolyte, m_{Fe} is the total dissolved iron concentration and m_H^{ref} corresponds to an empirical parameter for hydrogen ion diffusivity.

Measurements and calculations of the ionic conductivity for various solution compositions are shown in Table 2 and Fig. 4. Ionic conductivity decreases with increasing iron sulphate concentration in solution. This phenomenon is explained by the speciation model simulations, which indicate that the concentration of hydrogen ions (H^+) decreases by forming bisulphate ions (HSO_4^-) as iron sulphate is added to the solution. The ionic association degree increases with solute concentration, i.e. the relative amounts of Fe–SO_4 and H–SO_4 complexes increase if iron sulphate or sulphuric acid concentration increases.

Table 5
Standard diffusivities of ionic species at 25 °C

Species	Ionic diffusivity, D^0 m^2/s ($\times 10^{-9}$)
H^+	9.312 (Lide, 1999)
SO_4^{2-}	1.065 (Lide, 1999)
Fe^{2+}	0.719 (Lide, 1999)
Fe^{3+}	0.604 (Lide, 1999)
HSO_4^-	1.331 (Lide, 1999)
$Fe(SO_4)_2^-$	0.198 (estimated Eq. (11))
$FeSO_4^+$	0.201 (estimated Eq. (11))

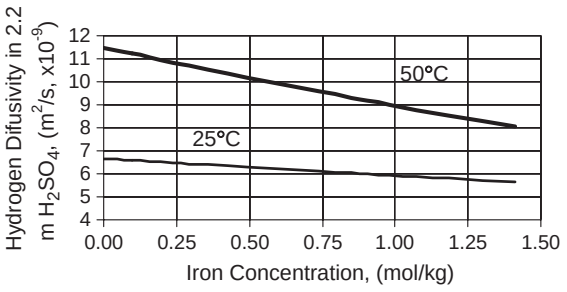

Fig. 5. Effective diffusivity of H^+ in 2.2 m H_2SO_4 aqueous solution at 25 and 50 °C, as a function of total dissolved iron concentration.

Fig. 4 shows that there is good agreement between experimental values and the values predicted by the presently developed speciation model. The standard deviation between experimental and calculated values was about 3–5% depending on solution composition. Greater differences were observed in more concentrated solutions.

Comparison of experimental and calculated results show that the model has been qualitatively and quantitatively validated, i.e. the predicted species distribution and solution concentrations are correct for Fe(II) and Fe(III) in aqueous solutions with 2.2 m H_2SO_4 in the 25–50 °C temperature range. Average parameters of Eq. (12) in aqueous solution with 2.2 m H_2SO_4 at 25 °C are: $D_{H+}=6.7\times10^{-9}$ (m^2/s) and m_H^{ref} 6.5 ±1.5 (mol/kg), and at 50 °C are: $D_{H+}=11.5\times10^{-9}$ (m^2/s) and $m_H^{ref}=3.7\pm0.3$ (mol/kg).

Fig. 5 shows the effective diffusivity of H^+ in 2.2 m H_2SO_4 aqueous solution at 25 and 50 °C, as a function of total dissolved iron concentration. A decrease in H^+ diffusivity was observed as iron concentration increased in solution. Hydrogen mobility was reduced by 15.6% and 30% at 25 and 50 °C, respectively.

Validation of the model could not be extended to a wider concentration range due to the considerable difficulties that were found in carrying out quantitative chemical analysis in high acidity solutions. The presented model includes long-range (electrostatic) binary interactions between anions and cations. The short-range interactions were evaluated as a function of the ionic strength of the solution using the simplified B-dot term as an extension of Debye–Hückel's model. Additional molecular, ion-solute and multi-ion interactions, which become significant at higher concentrations, are not included and require further work and the use of wider range models, such as the one proposed by Pitzer and co-workers (Pitzer, 1991). Establishing the

existence of other ionic and neutral iron–sulphate complexes requires further experimental work.

5. Conclusions

The experimental data and thermodynamic model described in this work allow the prediction of the speciation of the Fe(II)–Fe(III)–H_2SO_4–H_2O system at 25 and 50 °C. Calculations are in fair agreement with experimental data throughout the studied ranges.

Raman spectroscopy studies of aqueous solutions formed by mixtures of H_2SO_4, $FeSO_4^*7H_2O$ and $FeH(SO_4)_2$, show displacement of spectral bands with respect to pure species, indicating the existence of ionic interactions. This effect reveals the presence of bisulphate ions HSO_4^- and the complex $FeH(SO_4)_2^0$ in solution.

Free acidity decreases with the amount of dissolved iron in solution, indicating the existence of association between dissolved iron compounds and hydrogen ions (H^+), to form $FeH(SO_4)_2^0$.

Ionic conductivity increases with temperature, and decreases with increasing iron sulphate concentration due to the formation of bisulphate ions, which reduces the concentration of the more mobile H^+ ions.

Model simulations indicate that anions, cations and neutral complexes are present whenever the dominant species in the studied conditions are HSO_4^-, H^+, Fe^{2+} and $FeH(SO_4)_2^0$, which indicates that this solution presents a high buffer capacity due to the existence of bisulphate ions (HSO_4^-) as main species. A decrease in the concentration of H^+ and Fe^{3+} was observed as temperature increased, due to stability increase of HSO_4^- and $Fe(SO_4)_2^-$.

Comparison of experimental and calculated results shows that the model has been qualitatively and quantitatively validated, i.e. the predicted species distribution and solution concentrations are correct for Fe(II) and Fe(III) in aqueous solutions with 2.2 m H_2SO_4 in the 25–50 °C temperature range.

Finally, the following standard equilibrium constants for $FeH(SO_4)_2^0$ were obtained by using the thermochemical equilibrium model developed in this work: log $K_f^0 = 8.1 \pm 0.3$ at 25 °C and 10.0 ± 0.3 at 50 °C.

6. Notation

a	Activity, mol/kg
$\mathring{a}$	Ionic hard-core diameter, m
A	Debye–Hückel parameter, $kg^{1/2}/mol^{1/2}$
B	Debye–Hückel parameter
$\dot{B}$	B-dot parameter of the extended Debye–Hückel model, kg/mol
C	Molar concentration, $kmol/m^3$
D_{ef}	Effective diffusivity of the ionic species, m^2/s
F	Faraday's constant, 96,487 C/mol
I	Ionic strength, mol/kg
K	Equilibrium constant of formation reaction on a molal basis
m	Molal concentration, mol/kg
m_H^{ref}	Empirical parameter, mol/kg
NC	Number of solution components
NI	Number of ionic species in the solution
R	Ideal gas constant, 8.3173 J/mol K
T	Absolute temperature, K
TOT X	Total concentration, mol/kg
X	Concentration of a component, mol/kg
z_i	Charge number of ionic species

Greek letters

γ	Activity coefficient
κ	Solution conductivity, mS/cm
ν	Stoichiometric coefficient

Subscripts

a	Anion
c	Cation or component
f	Formation
i	Species subindex
j	Component subindex
s	Species
w	Water

Superscripts

0	Thermodynamic standard state

Acknowledgments

This work was funded by the National Committee for Science and Technology (CONICYT, Chile) via FONDECYT projects Nos. 1010138, 1030530 and the Universidad de Chile (project DID-1014-99/2). Support from both the Chemical Engineering and Mining Engineering Departments of the Universidad de Chile is gratefully acknowledged. The authors would like to thank Dr. Marcelo Campos-Vallette and Dr. Carolina Paipa for their help and collaboration in the interpretation of Raman spectrograms.

References

Allison, J.D., Brown, D.S., Novo-Gradac, K.J., 1991. MINTEQA2/PRODEFA2, A. Geochemical Assessment Model for Environmental Systems. Athens, GA, USEPA Report EPA/600/3-91/021.

Anderko, A., Lencka, M.M., 1997. Computation of electrical conductivity of multicomponent aqueous systems in wide concentration and temperatures ranges. Ind. Eng. Chem. Res. 36 (5), 1932–1943.

Baes Jr., C.F., Mesmer, R.E., 1976. The Hydrolysis of Cations. Wiley-Interscience, New York, pp. 370–375.

Baghalha, M., Papangelakis, V.G., 2000. High-temperature conductivity measurements for industrial applications: 2. H_2SO_4–$Al_2(SO_4)_3$ solutions. Ind. Eng. Chem. Res. 39, 3646–3652.

Barrett, J., Hughes, M.N., Karavaiko, G.I., Spencer, P.A. (Eds.), 1993. Iron speciation. In: Metal Extraction by Bacterial Oxidation of Minerals. Ellis Horwood Series in Inorganic Chemistry. Ellis Horwood Limited, Great Britain.

Butler, J.N., Cogley, D.R., 1998. Ionic Equilibrium Solubility and pH Calculations. John Wiley and Sons, N.Y., USA.

Casas, J.M., Alvarez, F., Cifuentes, L., 2000. Aqueous speciation of sulfuric acid–cupric sulfate solutions. Chem. Eng. Sci. 55 (24), 6223–6234.

Casas, J.M., Etchart, J.P., Cifuentes, L., 2003. Aqueous speciation of arsenic in sulfuric acid and cupric sulfate solutions. AIChE J. 49 (8), 2209–2220.

Casas, J.M., Papangelakis, V.G., Liu, H., 2005. Performance of three chemical models on the high-temperature aqueous $Al_2(SO_4)_3$–$MgSO_4$–H_2SO_4–H_2O System. Ind. Eng. Chem. Res. 44 (9), 2931–2941.

Cifuentes, L., Crisostomo, G., Alvarez, F., Casas, J.M., Cifuentes, G., 1999. The use of electrodialysis for separating and concentrating chemical species in acidic Cu–Fe–As–Sb electrolytes. In: Dutrizac, J.E., Ji, J., Ramanachandran, V. (Eds.), Electrorefining and Electrowinning of Copper. Fourth International Conference, Copper '99, vol. III. The Minerals Metals and Materials Society, Warrendale, Pennsylvania, USA, p. 479.

Cifuentes, L., Crisóstomo, G., Ibáñez, J.P., Casas, J.M., Alvarez, F., Cifuentes, G., 2002. On the electrodialysis of aqueous H_2SO_4–$CuSO_4$ electrolytes with metallic impurities. J. Membr. Sci. 207, 1–16.

Cifuentes, L., Glasner, R., Crisóstomo, G., Casas, J.M., 2003. Thermodynamics and kinetics of a copper electrowinning cell based on reactive electrodialysis. Copper 2003 International Conference, Santiago, Chile. November 30–December 3.

Das, S.C., Krishna, P.G., 1996. Effect of Fe(II) during copper electrowinning at higher current density. Int. J. Miner. Process. 46 (1–2), 91–108.

Dry, M.J., Bryson, A.W., 1988. Prediction of redox potential in concentrated iron sulphate solutions. Hydrometallurgy 21, 59–72.

Dutrizac, J.E., Harris, G.B. (Eds.), 1996. Iron Control and Disposal. Second International Symposium on Iron Control in Hydrometallurgy. October 20–23, Ottawa, Canada.

Dutrizac, J.E., MacDonald, R.J.C., 1974. Ferric ion as a leaching medium. Miner. Sci. Eng. 6 (2), 59–96.

Dutrizac, J.E., Monhemius, A.J. (Eds.), 1986. Iron Control in Hydrometallurgy. Ellis Horwood Limited, England.

Grenthe, I., Plyasunov, A., 1997. On the use of semiempirical electrolyte theories for the modeling of solution chemical data. Pure Appl. Chem. 69, 951.

Helgeson, H.C., Kirkham, D.H., Flowers, G.C., 1981. Theoretical prediction of the thermodynamic behavior of aqueous electrolytes at high pressures and temperatures: IV. Calculation of activity coefficients, osmotic coefficients, and apparent molal and standard relative partial molal properties to 600 °C and 5 kb. Am. J. Sci. 281 (10), 1249.

Herrera, L., Ruiz, P., Aguillon, J.C., Fehrmann, A., 1989. A new spectrophotometric method for the determination of ferrous iron in the presence of ferric iron. J. Chem. Technol. Biotechnol. 44, 171–181.

Langmuir, D., 1997. Aqueous Environmental Geochemistry. Prentice Hall, USA.

Lide, R.D. (Ed.), 1999. Handbook of Chemistry and Physics, 80th ed. CRC Press Inc., Boca Raton, Florida, USA.

Linke, W.F., 1958. Solubilities, Inorganic and Metal-Organic Compounds, 4th ed., vol. I. D. Van Nostrand Co, Princeton, N.J., USA.

Marconi, P.F., Meumer, V., Vatistas, N., 1996. Recovery of pickling effluents by electrochemical oxidation of ferrous to ferric chloride. J. Appl. Electrochem. 26, 693–701.

Nakamoto, K., 1997. Infrared Spectra of Inorganic and Coordination Compounds, 5th ed. John Wiley, USA.

Parkhurst, D.L., 1995. User's guide to PHREEQC—a computer program for speciation, reaction-path, advective transport and inverse geochemical calculations. US Geological Survey Water-Resources Investigations Report, vol. 95-4227. www.brr.cr.usgs.gov/projects/GWC_coupled/phreeqc.

Pitzer, K.S., 1991. Activity Coefficients in Electrolyte Solutions, Second edition. CRC, USA.

Rafal, M., Berthold, J.W., Scrivner, N.C., Grise, S.L., 1994. Models for electrolyte solutions. In: Sandler, S.I. (Ed.), Models for Thermodynamic and Phase Equilibria Calculations. Marcel Dekker, Inc., New York, USA, p. 601. Ch. 7.

Rao, S.R., Finch, J.A., Kuyucak, N., 1995. Ferrous–ferric oxidation in acidic mineral process effluents—comparison of methods. Miner. Eng. 8, 905–911.

Roine, A., 2002. HSC Chemistry for Windows: chemical reaction and equilibrium software with extensive thermochemical database. User's Guide, Version 5.0. Outokumpu Research Oy, Information Service P.O. Box 60 FIN-28101 PORI, Finland.

Ryzhenko, B.N., Shapkin, A.I., Bryzgalin, O.V., 1985. Electrolytic dissociation of metal sulfates in water solution. Geochem. Int. 22 (8), 5–11.

Senanayake, G., Muir, D.M., 1988. Speciation and reduction potentials of metal ions in concentrated chloride and sulphate solutions relevant to processing base metal sulfides. Metall. Trans., B, Process Metall. 19B, 37–45.

Shock, E.L., 1998. Slop98.dat, the upgraded thermodynamic database for the SUPCRT '92 Program, http://zonvark.wustl.edu/geopig/.

Sperry, E., Nagy, J., 1998. Electrolytic conductivity and resistivity measurements, In: Considine, D.M. (Ed.), Process Instruments and Controls Handbook, 3rd edition. McGraw-Hill, Singapore, pp. 6.137–6.154.

Stumm, W., Morgan, J.J., 1996. Aquatic Chemistry, 3rd ed. John Wiley and Sons, USA.

Swash, P.M., Monhemius, A.J., 1994. Hydrothermal precipitation from aqueous solutions containing iron(III), arsenate and sulphate. Hydrometallurgy '94 International Symposium. Institution of Mining and Metallurgy and the Society of Chemical Industry. Chapman and Hall, Cambridge, England, pp. 177–190. 11–15 of July.

Tozawa, K., Sasaki, K., 1986. Effect of co-existing sulphates on precipitation of ferric oxide from ferric sulphate at elevated temperatures. In: Dutrizac, J.E., Monhemius, A.J. (Eds.), Iron Control in Metallurgy. Ellis Horwood, Chichester, pp. 454–476.

Tremaine, P.R., Trevani, L.N., Rudolph, W.W., 2004. Acid–base ionisation and metal complexation under hydrothermal

conditions by UV-visible and Raman spectroscopy. In: Collins, M.J., Papangelakis, V.G. (Eds.), Pressure Hydrometallurgy 2004, 34th Annual Meeting of CIM, pp. 545–560. Banff, Alberta, Canada.

Welham, N.J., Malatt, K.A., Vukcevic, S., 2000. The effect of solution speciation on iron–sulphur–arsenic–chloride systems at 298 K. Hydrometallurgy 57 (3), 209–223.

Wolery, T.J., EQ3/6 Software Package, Version 7.2b, Lawrence Livermore National Laboratory, Livermore, CA. USA. 1996.

Zemaitis, J.F., Clark, D.M., Rafal, M., Scrivner, N.C., 1986. Handbook of Aqueous Electrolyte Thermodynamics. Design Institute for Physical Property Data-AIChE, New York, USA.